IMPACT OF VANE CLOCKING ON THE TEC LOSS IN RIG

M. Hoeger, R.D. Baier, A. Marn °, T. Selic °,
R. Niehuis [1], R. Gomes [1] Ch. Bode [2], J. Friedrichs [2]

MTU Aero Engines AG , D-80995 Munich, Germany, Email: martin.hoeger@mtu.de
° Institute for Thermal Turbomachinery and Machine Dynamics,
Graz University of Technology, A-8010 Graz, Austria, Email: andreas.marn@tugraz.at
[1] Institute of Jet Propulsion, Universität der Bundeswehr München,
D-85577 Neubiberg, Germany, Email: reinaldo.gomes@unibw.de
[2] Institute of Jet Propulsion and Turbomachinery, Technische Universität Braunschweig,
D-38108 Braunschweig, Germany, Email: chr.bode@tu-braunschweig.de

ABSTRACT

The 30% span profile section of the H-TEC highly loaded Turbine Exit Casing was transformed into a plain cascade configuration with identical pressure distribution and loading level. At increasing levels of complexity the incompressible flow in cascade is studied first at different inlet turbulence levels at the Technische Universität Braunschweig. Unsteady inlet conditions were then generated using rotating bars at the cascade wind tunnel of the Armed Forces University Munich at compressible flow speeds and varying Reynolds numbers. Finally the TEC configuration is investigated in the TU Graz STTF 1.5 stage turbine rig using a conventional 5-hole-probe, a miniature Pitot-probe and a hot wire anemometer. A special test- and evaluation concept allows for highly accurate data.

The results show a strong vane-TEC clocking, which for the TEC total pressure inlet profile may be approximated by a sine-function. Downstream the TEC, between the wakes, still a sinus shaped total pressure variation is found. Two loss coefficients are evaluated (i) by a classical control volume approach between TEC inlet and exit plane and (ii) by a so-called viscous wake approach. This method compares the viscous flow in the wake region with a hypothetical potential flow deduced from the flow in the same exit plane between the TEC wakes. The viscous wake method compared at 30% span quite nicely to the cascade data. However, the control volume approach yields more than twice the cascade loss, which indicates further loss sources to exist, e.g. unsteady losses to rise from a vane wake - rotor - TEC interaction or turbulence to impact the probe reading.

KEYWORDS

LPT exit guide vane, TEC, vane clocking, unsteady losses

NOMENCLATURE

Indices and Abbreviations

AR	aspect ratio AR=H/c, H passage height	Ma_1	inlet Mach number
av	mass averaged quantity	PHI/g	normalized circumferential coordinate
c, cax	chord, axial chord	Pit	Pitot probe
cp_{1c}	pressure coefficient, see eq. (1)	Pot	quasi potential flow
cv	control volume loss evaluation	Pt, p	total pressure, static pressure
EIZ+40	wake generator (moving bars)	q	dynamic head q = Pt-p
EIZ_st	steady case (without bars)	Re_1	Reynolds number
g	pitch	sin all	sinus approx. quasi pot. flow all pitch

sin loc	sinus approx. quasi pot. flow at wake
spline	evaluation using spline function
Sr	Strouhal no. $Sr=(V_\varphi/g)_{Rot}\cdot(cax/U)_{TEC}$
TEC	Turbine Exit Casing (exit guide vane)
Tu	turbulence intensity $Tu=(u'^2)^{0.5}/U_o$
TUBS	Technische Universität Braunschweig
TUG	Technische Universität Graz
5HP	5-hole probe (standard probe)
1, 2	TEC inlet, exit ref. planes, see Fig. 2

Greek

$\Delta x/cax$	rel. axial gap with cax upstream
δp_1, δPt_1	inlet pressure corrections, eq.(1)
U, U_o	axial velocity, main speed
UniBwM	Univ. of the Armed Forces Munich
vw	viscous wake (profile) loss evaluation
V_φ	rotor or EIZ-bars angular speed
Xi	loss coeff. $Xi=(Pt_1-Pt_x)/Pt_1$
Zv_1	loss coeff. $Zv_1=(Pt_1-Pt_x)/(Pt_1-p_1)$

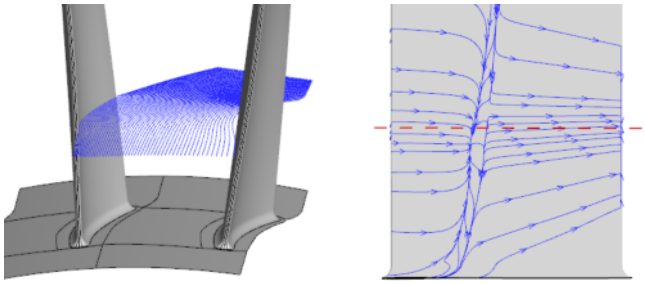

Figure 1: Rotat. symmetric streamsurface (left), Q2D suction surface streamlines (right). H-TEC simulation close to 30% span

INTRODUCTION

In modern jet engines the boundary conditions of the turbo components are often impacted by strutted transition ducts. For a low pressure turbine (LPT) inlet conditions may be generated either by a non-turning strut followed by a vane or by a Turning Mid Turbine Frame. Downstream the LPT the Turbine Exit Casing (TEC) is found, with guide vanes to remove residual swirl and to generate homogeneous exit flow. The TEC may be understood as a diffusor, which in upstream direction transforms ambient pressure into lower turbine back-pressure, and by that sets the exit boundary conditions to the LPT. An encouraging approach to shift TEC loading limits towards lower solidity is given by Kurz et al. (2017) using pulsed blowing. Highest efficiencies are achieved with optimum boundary conditions and it is clear that the precise understanding of strutted duct flow is important.

Several papers address strutted transition duct flow. Marn et al. (2009) investigated the flow through an s-shaped intermediate turbine duct with integrated turning struts downstream of an transonic HP turbine stage. Santner et al. (2011) presented the flow evolution through such a duct and the influence of a counter rotating LP turbine downstream of the duct. Göttlich (2011) summarised the research regarding duct flows in his review paper. Clocking effects have been studied by Schennach et al. (2007) and (2008). However, little is said about the special flow conditions under which TEC ducts operate and about the problem not only to find out the best design, but to elaborate accurate data for validation. Only with codes carefully validated the optimum LPT-duct combination can be found in the early design phase, with neither taking valuable acceleration from the LPT by a duct underloading, nor creating an undesirable duct overloading with the hazard of efficiency penalties from flow separation.

The present paper addresses the special TEC inlet flow situation on the basis of TU Graz 1.5 stage STTF-rig results. The experimental set-up allows for highest accuracies and consistent data. Michelassi et al. (2015) use DNS and LES simulations to calculate mixed out losses for a turbine cascade with unsteady inlet conditions. By subtracting from the total loss the calculated profile loss according to a formula of Denton (1993), the unsteady loss component is obtained. In the present paper a special 2D rotationally symmetric flow situation at 30% span is used to evaluate the profile loss found in the wake region against a hypothetical potential flow between the TEC wakes at exit. This loss compares quite well with steady and unsteady cascade data. Losses evaluated for the control volume between TEC inlet and exit are more than two times higher and contain the unsteady loss component. High vane loadings upstream the TEC are demonstrated to cause a strong vane wake-TEC clocking effect on the basis of time averaged probe data. Unsteady hot wire measurements had been performed late in a second measurement campaign. Only limited information on turbulence intensity is available in this paper.

TEC DESIGN

The investigations are performed at 2 linear cascade wind tunnels and in a 1.5 stage rig with constant radii at hub and tip. By that, at a reduced number of parameters, 2D and 3D flow phenomena may be better distinguished. To further shift TEC loading limits, a moderately loaded acoustic design, called Inverse Cut-Off or I-TEC, see Schönleitner et al (2014) and Marn et al. (2015), was aerodynamically optimized. Result was a new highly loaded TEC design, the so-called H-TEC and a linear H-cascade with the same pressure distribution and loading level as the 30% span section of the H-TEC. For geometric and aerodynamic parameters from pre-test simulations see Tab. 1. Note maximum inlet Mach number for cascade tests with 0.35 to be chosen at the upper end of the incompressible flow range to enable a sound code validation as well as a good comparison with rig data.

test facility/	location	Ma1	Re1	Sr	c/g	Tu1	AR	α1
config		-	10e-5	-	-	%	-	deg
TUBS H-casc	mid sect	0.07	1.5	-	1	0.6/ 2.1	3	28.2
UniBwM H-casc	mid sect	0.35	1.5	0.46	1	2.0	1.6	28.2
TUG rig H - TEC	30 %span	0.23	1.35	2.1	1	5.5	2.162	30.4

TUG STTF rig	IGV	V1	B1	I-TEC	H-TEC
blade no.	83	96	72	> 40	32
axial gap Δx/cax %	375	73	195	-	-

Table 1: Aerodynamic and geometric parameters of cascades and rig TEC experiments

SIMULATIONS

3D NAVIER STOKES (RANS)

MTU/ DLR TRACE solver is used. A number of 9 million nodes with k=117 in radial direction was used to simulate the whole rig flow with 2 million nodes used to accurately resolve the TEC duct. First grid line was at a wall distance y+ between 0.5 and 1. Fillets, IGV cantilevered hub gap and rotor tip gap are resolved by the CFD mesh in radial direction with k= 25 and 21 nodes, respectively. No cavities are included in the simulations. Turbulence modelling was according to Wilcox 1988 with pressure surfaces fully turbulent and suction surfaces with transition. Only the TEC was run with transition active on both surfaces. Transition model was Multimode of Kozulovic (2007).

TEST CONCEPT

The geometry of all blading (LPT-stage, TECs, cascades) had been checked by white light scans to ensure rotationally periodicity to be kept. Repeatability had been demonstrated at the main rig operating point in an earlier test campaign. Identical cascade blading was used for both wind tunnel test campaigns.

2D flow conditions at H-TEC 30% span from RANS simulations are shown in Fig 1 and will be confirmed by measured constant total pressure surfaces in the chapter on measured 3D traverse data and close to 2D flow on the suction surface at 30% span in chapter on flow visualization.

Cascade Testing

Windtunnel oft the Technische Universität Braunschweig

The experimental investigations at Technische Universität Braunschweig were carried out in the low speed cascade wind tunnel of the Institute of Jet Propulsion and Turbomachinery. Details of the experimental facility are described by Ackermann (1956). The experiments were carried out at fixed Mach and Reynolds number for varying turbulent inlet conditions and inlet flow angles according to Table 1.

The evaluation of the measured data has been done according to Fischer (2011). Uncertainty analysis yields maximum value of 2.3% for the total pressure loss and pressure rise coefficient, 2.2% for turning angle and 0.4% for the static pressure coefficient cp1, Nerger (2009). Based on the

Figure 2: Meridional section of the STTF-AAAI rig (bottom), measurement planes (top, right)

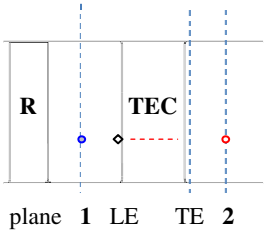

location	plane	Δx/cax
TEC inlet	1	0.83
TEC TE	TE	0.03
TEC exit	2	0.55

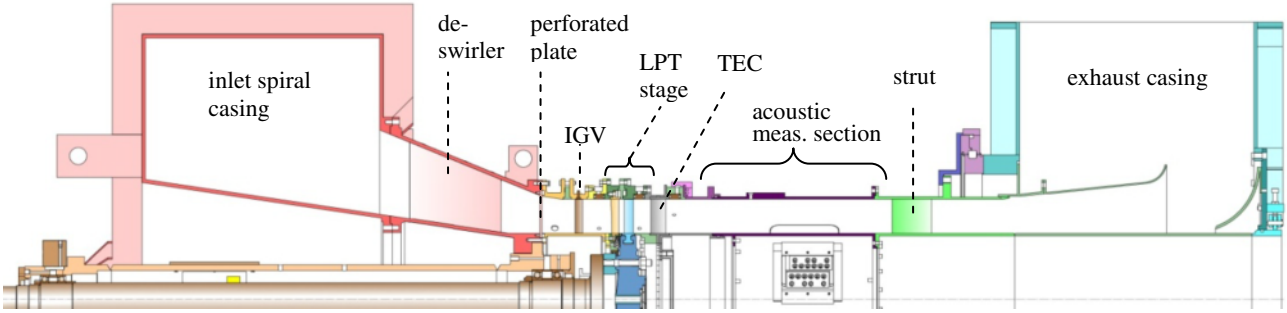

good reproducibility of the oil flow pictures an uncertainty for the flow visualization can be neglected. The turbulence intensity at inlet varies within a range of 0.1%.

Windtunnel of the University of the German Federal Armed Forces Munich

The High-Speed Cascade Wind Tunnel at the German Federal Armed Forces University Munich is an open loop test facility running at realistic Mach numbers up to Ma=1 at the nozzle exit. The main parts of the tunnel including the test section are enclosed inside a pressure tank which allows to change the static pressure at the cascade in- and outlet. This feature allows to change the Reynolds number independently from the Mach number, both at typical levels for turbomachines. Detailed descriptions of the facility can be found in Sturm and Fottner (1985) or Kurz et al. (2017).

Periodically unsteady inflow conditions are generated by moving cylindrical bars upstream of the cascade. The bars move parallel to the cascade upstream of the cascade and generate similar wakes as upstream moving aerofoils. The design is explained in Acton and Fottner (1996).

Rig Test

TU Graz STTF-AAAI rig

The Institute for Thermal Turbomachinery and Machine Dynamics at Graz University of Technology operates a 3MW compressor station in order to supply a couple of test facilities continuously with pressurized air. In the described subsonic turbine test facility for aerodynamic, acoustic and aeroelastic investigations (STTF-AAAI) the maximum pressure ratio is limited to 2 due to the inlet spiral casing. The maximum mass flow rate is 15 kg/s at a temperature at stage inlet of 100 °C. This inlet temperature can be adjusted by coolers within a wide range. The pressurized air enters the facility through a spiral inlet casing where the flow turns into axial direction. Within this spiral inlet casing the front bearing of the overhung-type turbine shaft is mounted. The shaft is coupled to a water brake, whose cooling water cycle is connected to the re-cooling plant of the institute. In order to provide well defined and uniform inflow conditions a de-swirler together with a perforated plate is located upstream of the stage inlet. Further, upstream of the stage (and downstream of the perforated plate) inlet guide vanes can be found that should simulate additional wakes of other upstream low pressure turbine stages. The air leaves the rig through an acoustic measurement section, supporting struts, exhaust casing, and the exhaust stack to ambient, see Fig. 2. A detailed description of the STTF-AAAI is given in Moser et al. (2007).

The aerodynamic design of the low pressure turbine stage, IGVs as well as the EGVs was performed by MTU Aero Engines. Considerable effort was put into the adjustment of relevant model parameters to reproduce the full scale LPT configuration. The turbine diameter is approximately half of that of an aero engine LPT and therefore the rig is operated at higher

rotational speeds. A meridional section of the rig is shown in Fig. 2, bottom, for an enlarged view of the H-TEC with reference plane locations see Fig 2, top, right. The blading is not drawn to scale. The rig is characterised by a high aspect ratio unshrouded rotor followed by the EGVs of the TEC.

Reference Planes:

To achieve highest accuracies three TEC vanes are instrumented with Kielheads at nine radial leading edge stations. Every total and static pressure measurement is normalized with the average Kielhead value to take into account different ambient conditions as well as the impact of tiny variations in speed and flow on the pressure reading. For ADP conditions within a measurement campaign fairly constant average reference pressures are observed.

In Fig. 2, top, right 30% span measurement locations at the reference planes are indicated. A blue circle shows inlet reference plane 1, leading edge Kielhead is given by a diamond symbol and exit reference plane 2 by a red circle at $\Delta x/cax=0.55$. Cascade exit reference plane locations are with $\Delta x/cax= 0.33$ (TUBS) and 0.40 (UniBwM) far enough downstream the trailing edge in mixed out 2D wake flow not to impact losses and to allow a sound comparison with rig data.

Blade Row Loss Breakdown

Compared to standard turbine blading, the struts at the inlet and exit o f a LPT are characterised by a lower turning and lower Mach numbers. Two definitions for the loss coefficient are investigated: at close to incompressible speeds the loss coefficient $Zv_1=\Delta Pt/q_1$ is known to be independent of the Mach number and may be used as a blade quality criterion. The second definition $Xi=\Delta Pt/Pt_1$ gives the actual loss in total pressure relative to its inlet value. In Fig. 3 for the present rig calculated RANS data are normalized with vane loss. The TEC loss coefficient Zv_1 amounts 56% of the LPT-Vane value, while for the definition Xi only 18% vane loss is found for the TEC. In other words, the relative loss in total pressure generated in the stator vane is more than 5 times higher than that in the TEC. Compared to the calculated steady LPT-vane loss, already an 18% loss increase from unsteadyness and vane wake-TEC interaction would double the losses between rotor and TEC exit.

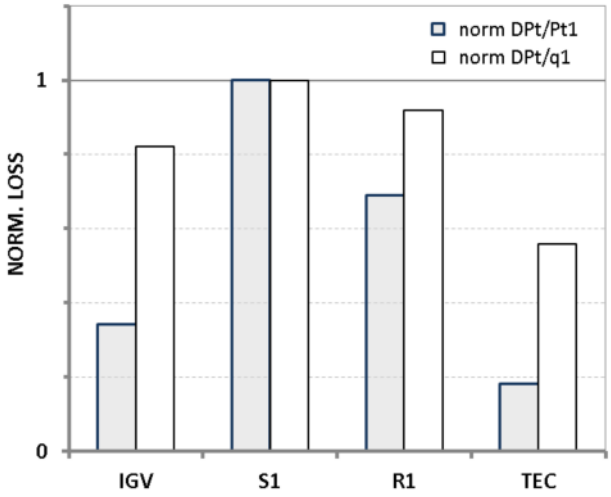

Figure 3: Normalized rig blade row loss coeff. based on dynamic head vs. based on total pressure.

EXPERIMENTAL RESULTS

Only ADP data are presented.

Pressure Distributions

As boundary layer loading is impacted most by pressure gradient, pressure distributions are discussed first. At inlet Mach numbers between 0.069 and 0.35 little compressibility effects are expected for the coefficient $cp_1=(p_x-p_1)/(Pt_1-p_1)$. To best compare pressure gradients on suction surface, correction terms are introduced e.g. to account for small circumferential variations in reference total pressure between leading edges instrumented with Kielheads and TEC vanes with surface static pressure tappings or the impact of turbulence on the pressure reading by eq. (1):

$$cp_{1c} = \frac{p_x - (p_1 - \delta p_1)}{(Pt_1 + \delta Pt_1) - (p_1 + \delta p_1)} \qquad \text{eq. (1)}$$

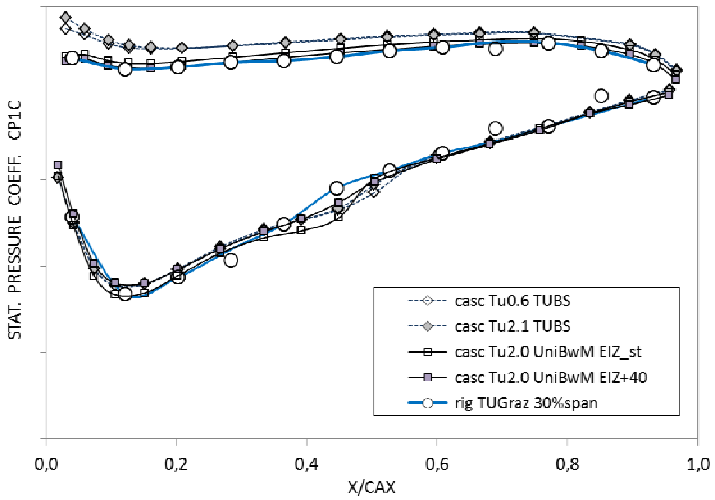

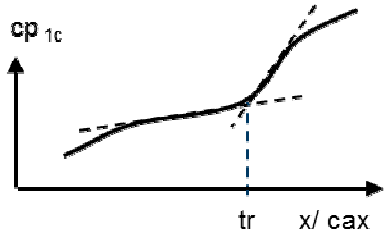

Figure 4: Static pressure distributions (left) H-TEC cp_{1c} at 30% span vs. 2D cascade data. (top) Sketch of transition loc estimate (tr) by two tangents.

Fig. 4, left, shows a comparison of cp_{1c} H-cascade data for both wind-tunnels. No corrections in $\delta Pt/Pt$ and $\delta p1/p1$ are applied for the cascade data.

Cascade Inlet Turbulence

A separation bubble with transition from laminar to turbulent is seen on the suction side, which decreases in length by about 5 % chord with inlet turbulence Tu_1 increasing from 0.6 to 2 %. For transition onset detection from two tangents see sketch in Fig. 4, right. Deviations found on the pressure side between data of the two wind tunnels may be explained from deviations in aspect ratio and Mach number. With unsteady inlet conditions added, the transition bubble is nearly removed, Fig. 4, left, and only a small plateau in the cp-curve indicates that transition on suction side may have taken place earlier at about 40% chord.

Rig Data

H-Cascade midsection pressure distribution was designed to meet H-TEC 30% span rig data at ADP. To best compare rig with cascade cp-data, measured results given in Fig. 4, left are corrected by a small amount in $\delta p_1/p_1$ = 0.05%. The application of a turbulence correction $\delta Pt/Pt$ due to Appendix A1 did not significantly impact the pressure coefficient cp_{1c}. At similar suction side cp_{1c} shape and gradient transition location may be detected at about 5% chord further upstream in the rig. However, as number of tappings is limited in rig, transition may be best discussed together with flow visualisations in the following chapter.

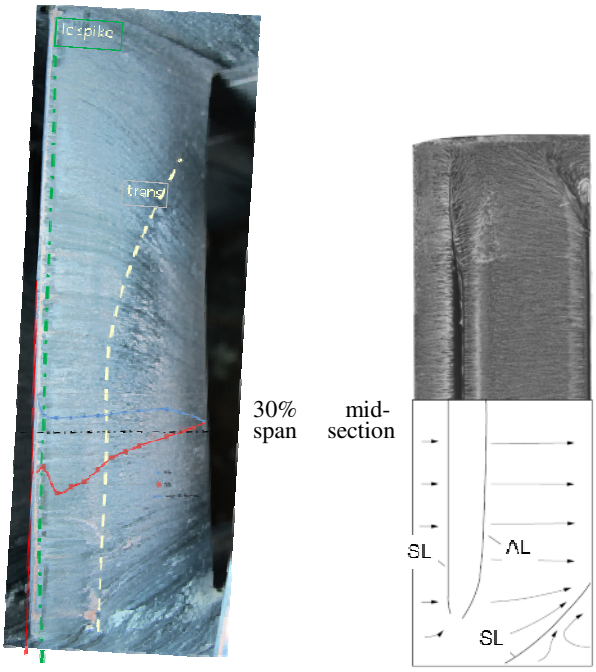

Figure 5: Flow visualization on suction side. H-TEC (left) vs. H-cascade (right)

Flow Visualisation

A mixture of dye, oil, and paraffin is used to visualize boundary layer flow. The dye spreads on the surface under the impact of wall shear, pressure gradient, and inertia forces. For the H-cascade straight streaklines are visualized at the mid section, Fig. 5, right, with a separation bubble found from laminar separation line SL followed by a turbulent re-attachment line AL. In the rig at 30% span a leading edge spike is visualized, see cp-distribution in Fig. 5, left. No pronounced separation bubble is visible on the suction side

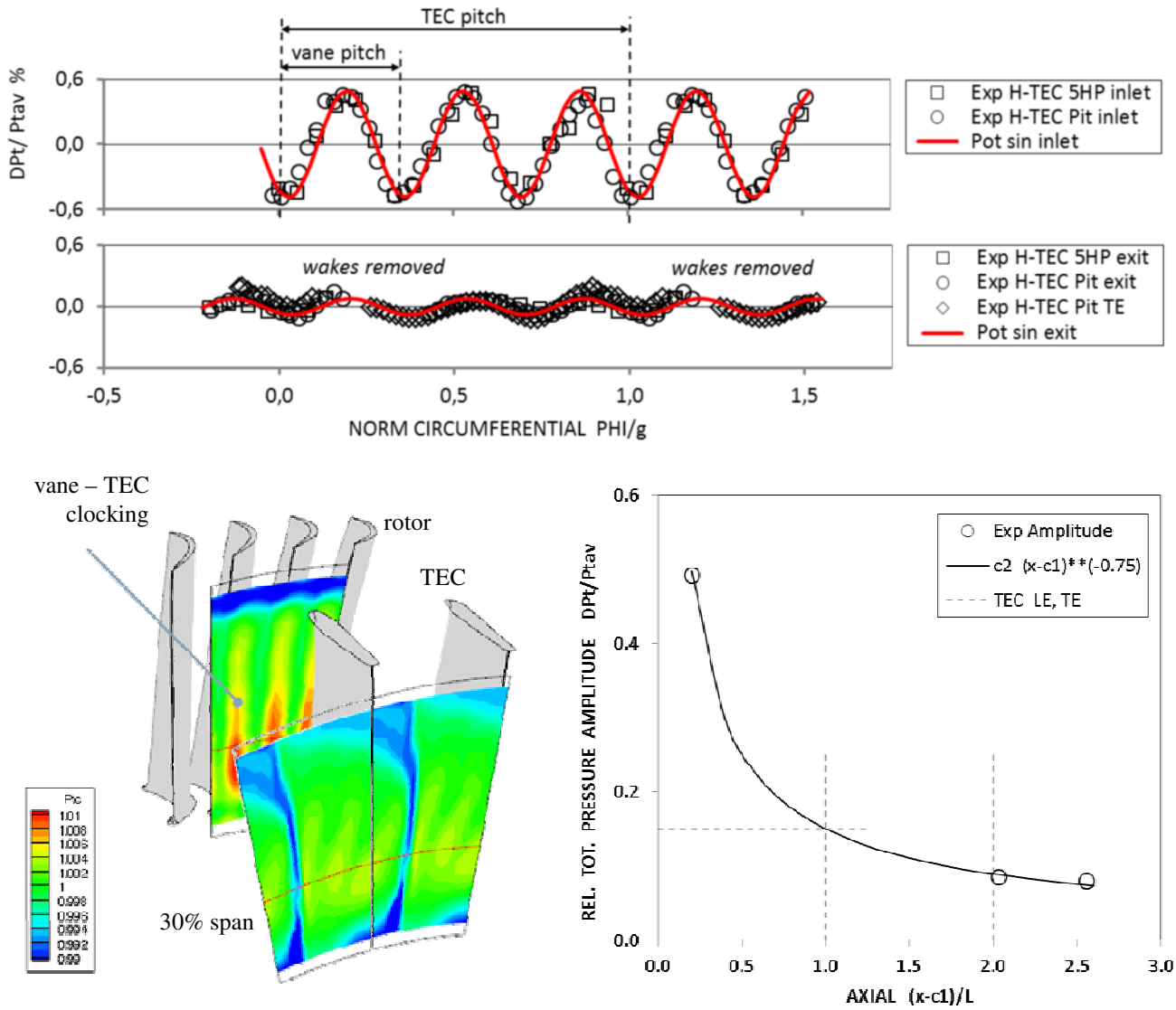

Figure 6: (left) Measured total pressure contours H-TEC inlet and exit plane (top) Total pressure quasi potential flow H-TEC at 30% span, inlet and exit

(right) Decay of total pressure amplitude, experiment vs. short cut formula

and natural transition takes place close to a low shear region. This result is in line with the transition location already observed in the pressure distribution shown in Fig. 4, left and the flow visualization in Fig. 1, right.

3D Rig Traverse Data

Measured total pressure contours are given for H-TEC inlet and -exit planes in Fig. 6, left. Assuming periodicity in the exit plane, the 5HP- data are repeated for the neighbour passage to best resolve flow for the wake region. The clocked vane wakes are clearly visible between high pressure regions shown in red and yellow in the TEC inlet as well as in the TEC exit plane. Fairly 2D flow conditions without radial gradients are confirmed for the 30% span locations, see red dashed lines in Fig. 6, left. At this location for a 5% span radial shift the mass averaged measured total pressure increase was in the order of 10% TEC profile section (cv) loss, i.e. a possible streamline shift between reference planes 1 and 2 will not dominate the loss calculated by a 2D control volume approach.

2D Rig Traverse Data at 30% Span

TEC Inlet:

The circumferential variation in normalized total pressure at TEC inlet is given in Fig. 6, top, for 5-hole- and Pitot probe data. A sine-function is found to fit well with little impact of probe type or TEC configuration. At excellent periodicity the wavelength is linked to the vane number, i.e. three vane wakes occur on one H-TEC pitch. A large amplitude of about ± 0.4 % average total pressure is found, which may be transformed into a loss coefficient ΔPt/Pt = 0.4% looking on maximum pressure data as a region of undisturbed flow.

This estimate indicates vane wakes after being turned, sheared and diffused in the rotor passages still to show a loss in the order of the vane loss itself, for basic unsteady interaction mechanism see e.g. Eulitz et al. (1996) or Stieger and Hodson (2004). Actually vane losses are not only convected downstream but in addition modify work extraction in the rotor, see Evans and Longley (2016b).

TEC Exit Potential Flow:

Normalized total pressure data measured with two probe types in reference exit plane downstream and close to the TEC trailing edge are given for the two TEC configurations in Fig. 6, top. With data points in the wake region removed, the measurements are again surprisingly good approximated by a sine function with an amplitude of ± 0.08 %. The approach to discard data at the edge of the wake, which do not follow a sine function seems to be rather rude. However, it is instructive for a TEC with comparatively low turning to observe a potential flow region to exist impacted by vane wakes and nearly unaffected by the distance of the plane to the trailing edge.

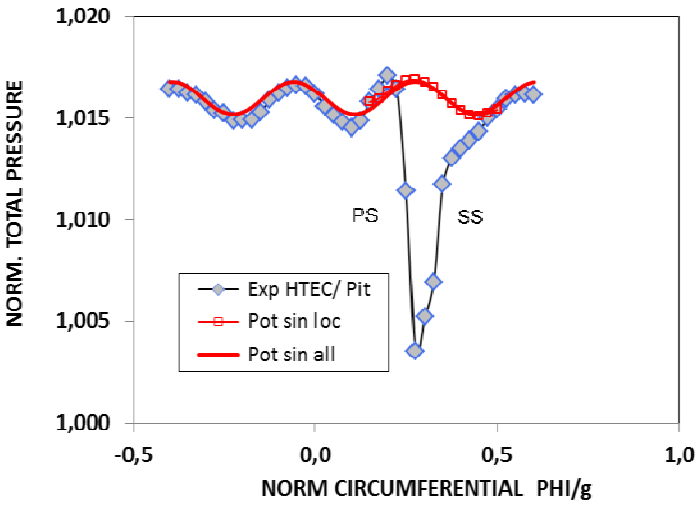

Figure 7: H-TEC Pitot-probe data at 30% span with potential flow assumption (red squares)

Following a short cut formula given in Schlichting [1965] p.687, the mixing of a free jet may be correlated by $\sim x^{-2/3}$ for a 2D wake by $\sim x^{-1}$. In the present case an exponent of 0.75 was found to best approximate the total pressure amplitude for the three measurement planes. Neglecting wake-TEC interaction an approximate decay of the vane wake amplitude may be found in Fig. 6, right, with two constants c1 and c2 introduced to adjust to the present case. Due to the simple power law assumption close to the TEC leading edge the mixing process is nearly completed and only a small change in amplitude is expected in the TEC passage and the exit flow.

Viscous Wake Loss

Although the interaction of the incoming rotor and stator wakes with the TEC boundary layers permits a clear separation of TEC wake region and potential flow, the viscous losses in the TEC-wake region may be compared to a circumferentially periodic quasi potential flow to calculate a so-called viscous wake loss coefficient. By that, measured wake shapes, which at the first sight look erroneous, are understood as a result of vane wake clocking. In the present case for the H-TEC a total pressure minimum occurs at the suction surface edge of the wake, see Pitot data in Fig. 7.

Mass-averaged total pressures may be calculated for the wake traverse data and for the quasi potential flow using the average measured exit flow angles and static pressures from measurement. By that, highly accurate losses are evaluated with any loss source or measurement deviation found

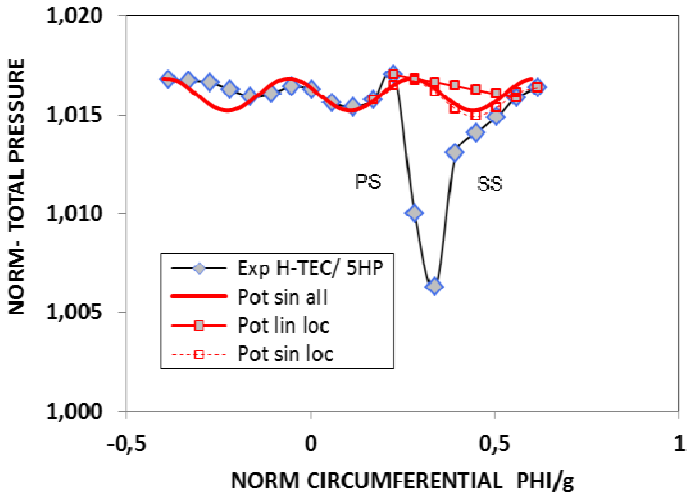

Figure 8: Potential flow assumptions. H-TEC 5HP data 30% span

probe type/ pot flow approx	ΔZv_1 % ref
Pit/ sin loc (ref)	0.0
Pit/ spline sin loc	-1.0
Pit/ sin all	15.6
Pit/ lin loc	8.4
5HP/ sin loc	-9.7
5HP/ spline sin loc	-12.1
5HP/ sin all	-11.2
5HP/ lin loc	10.4

Table 2: Deviation in loss coefficient from pot. flow assumptions. H-TEC 5HP and Pitot data 30% span

outside the TEC-wakes not taken into account. In a similar way CFD data may be evaluated for validation issues. Different quasi potential flow assumptions have been studied, see Fig. 8:

(1) Pt linear in the wake region, range determined from velocity gradient based cut-off, see Khalid et al. (1998), outside wake region use data as measured
(2) full sine function for the whole pitch, adjusted to meet Pt-data outside the TEC-wake
(3) part sine function combined with linear in wake region, range determined from smooth transition to measured data, outside wake region use data as measured

The H-TEC 5HP data in Fig. 8 show some deviations from the sine-function for the quasi potential flow region. The three evaluation methods given above are best investigated for this case. The results in Tab. 2 show for 2 probe types and 3 evaluation methods a surprisingly low scatter in the range of +/- 15%. Method (3) was selected because it's smooth transition from potential flow to the measured data. Using a spline integration instead of a linear variation between data points changed the result only by 1%. Method (2) interprets all deviations from the sine-curve as loss contribution. Method (1) does not distinguish between potential flow induced gradient (vane clocking) and the wake flank gradient. The viscous wake formula has the advantage of being applicable locally in any close to 2D flow and it uses data from a single measurement campaign only. Provided a region with quasi potential flow to exist, the interaction of the rotor wakes with the TEC boundary layers are approximately kept by the method.

Losses from Control Volume

A standard integration was applied using 30% span data normalized by inlet total pressure from leading edge Kielhead probes. Similar to Evans and Longley (2016a) too high inlet total pressures are observed compared to the simulations (not shown here). Besides the impact of inlet unsteadiness on the probe reading, see Appendix A1, the unsteady mixing and interaction of the vane wakes as well as losses from rotor wake TEC interaction have to be taken into account. Michelassi et al. (2015) find for a turbine cascade an additional unsteady loss in the order of 100% steady loss. Although the TEC turns the flow only 25% of the value of this turbine cascade, it's lower loss level (only 18% Xi rig vane) and the diffusing main flow makes it more sensitive to unsteady losses.

Loss Comparison

TEC loss coefficients Zv_1 normalized with H-cascade unsteady result are compared over Reynolds number in Fig. 9. Data from TEC inlet and exit measurement planes are shown and only a single result (not fully valid from the probe being too close to the trailing edge) is presented for the trailing edge plane.

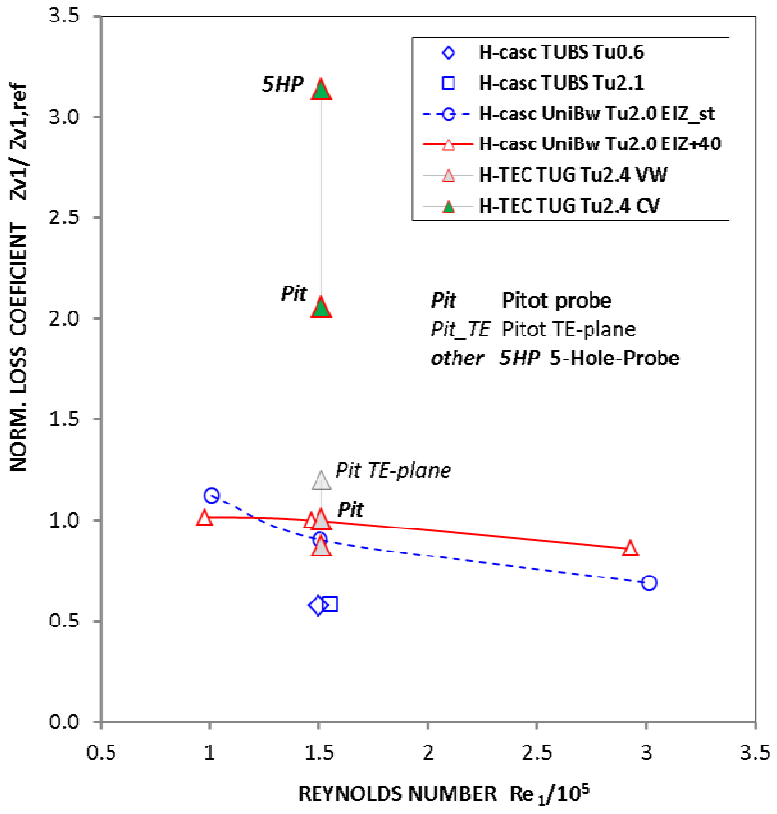

Figure 9: Impact of turbulence and unsteadiness on 2D loss. Cascade midsection vs. 30% span rig-TEC

Cascades:

Inlet turbulence intensity was investigated at Technische Universität Braunschweig, see Koch et al. (2012). Little impact of inlet turbulence was found for Tu_1 = 0.6 and 2.0 at incompressible speeds. Somewhat higher losses are measured at Armed Forces University Munich for Tu_1 = 2.1 and Ma_1=0.35. Here the lower aspect ratio from test set-up for rotating bars (EIZ_st: no bars installed) leads to earlier transition and an increased pressure gradient at the turbulent re-attachment location on the suction surface, compare Fig. 4, left. To simulate unsteady inlet flow, rotating bars are applied (EIZ+40: with moving bars). The lapse rate now gets less sensitive to the Reynolds number with losses at design conditions close to the steady inlet flow case. This result suggests rotor-TEC interaction in the present case to be less important.

Rig 30% span

The viscous wake evaluation (vw) for the Pitot data exactly meets the unsteady cascade result, while the 5HP data show slightly lower losses. The unfavourable pressure gradient from vane wake-TEC clocking seems not to play a major rule in loss production. For consistency the viscous wake (vw) result in the trailing edge plane is added in Fig. 9. Situated only 1 mm downstream the trailing edge, a slightly higher loss compared to the reference TEC exit plane is found.

More than twice the loss from viscous wake (vw) evaluation is evaluated with the control volume approach (cv) with a strong impact of the probe type in the rotor exit flow. This result indicates unsteady losses to be generated either from vane-wake and rotor-wake-TEC interaction as well as from vane wakes mixed out and diffused in the TEC passage. It should be kept in mind that turbulent spots and pressure gradients from vane wakes will show higher variations in time compared to the time averaged variations found in circumferential direction from conventional probe data.

While the viscous wake results from the two probe types agree quite well, the 5-hole result elaborated for a control volume method is considerably higher than the one from the miniature Pitot-probe. Similar sine-shaped total pressure curves are shown for the two probe types in Fig. 6, top with only the average values to differ. However, for the TEC inlet measuring plane the relative

distance Δx/cax to the rotor trailing edge is 83% cax, which would allow for mixed out 2D rotor wakes in steady 2D flow. Furthermore in Bauinger et al. (2017) the 5-hole-probe reading is demonstrated not to be compromised by turbulence.

CONLUSIONS

A linear cascade is designed using the 30% span section of a LPT-Rig TEC with low solidity. Fairly 2D potential flow is found at 30% span in the rig. At increasing levels of complexity the impact of turbulence, Reynolds number, and unsteadiness is first studied in cascade. In a next step the cascade midsection data are compared with rig results at 30% span to work out the impact of unsteadiness and clocking found in the rig.

A special test concept for highest accuracies is necessary to generate data with absolute accuracy for code validation issues. Here a leading edge Kielhead instrumentation for reference total pressure together with a miniature Pitot probe in combination with a five-hole-probe was applied successfully. A new loss evaluation method is proposed, which compares a periodic alternating quasi potential flow with the total pressure defect in the TEC wake. Such a quasi potential flow is demonstrated to exist still downstream the TEC between the TEC wakes and it is for the present rig test fairly well approximated by a sine-function with vane number as frequency. For this potential flow it was presupposed a region unaffected by TEC-wakes to exist. The measurements confirm this assumption for the comparatively low turning and low solidity found in TEC. The results obtained from this so-called viscous wake method compare good with measured 2D cascade compressible data.

Losses from a classical control volume evaluation contain the TEC profile losses as well as unsteady losses from rotor- and vane wake-TEC interaction in the flow passage upstream and between the TEC profiles. Furthermore unsteadiness and turbulence downstream the rotor impacts the probe reading. More than 150% higher TEC losses are evaluated, which may justify the partly rude assumptions made for the viscous wake approach.

Sinus-shaped total pressure variations stemming from the interaction of the vane wakes with the rotor flow have been found at TEC inlet in spanwise direction. Looking on these low total pressure regions as a pure loss, a several times higher total pressure defect (losses convected into the TEC passage) is found compared to the TEC steady 2D loss itself. This finding indicates the amount of unsteady losses found upstream and in the TEC passage have to be judged in the spirit of the blade row they originate from (vane and rotor wakes) and not compared to the comparatively low loss level found for the TEC.

For other type of blading with different vane clocking features the quasi potential flow may be approximated better by a Fourier transformation. At higher loading levels, solidities and closed stagger angles the profile wake region may more and more dominate the whole exit flow field and no region with quasi potential flow may be found anymore.

ACKNOWLEDGEMENTS

This program has been supported within LuFo 4/3 by the German Ministry of Economics under grant number 20T0904A.

REFERENCES

Ackermann, E. (1956). *Eichmessungen am Kleinen Gitterwindkanal*. Bericht 56/17. Institut für Strömungsmechanik der Technischen Hochschule Braunschweig.

Acton, P. and Fottner, L. (1996) The Generation of Instationary Flow Conditions in the High-Speed Cascade Wind Tunnel of the German Armed Forces University Munich. In 13th Symposium on Measuring Techniques. Zurich, Switzerland.

Bailey, S. C. C., Hultmark, M., Monty, J. P., Alfredsson, P. H., Chong, M. S., Duncan, R. D., Fransson, J. H. M., Hutchins, N., Marusic, I., McKeon, B. J. , Nagib, H. M., Örlü, R., Segalini, A., Smits, A. J., Vinuesa, R. (2013). *Obtaining accurate mean velocity measurements in high Reynolds number turbulent boundary layers using Pitot tubes*. J. Fluid Mech. (2013), vol. 715, pp. 642_670.

Bauinger, S., Marn, A., Peters, A., Göttlich, E., Heitmeir, F. (2017). *Influence of Pressure Fluctuations on the Mean Value of Different Preumatic Probes*. paper ETC2017- 325, to be presented on 12th European Turbomachinery Conference, 3.-7. April 2017 Stockholm, Sweden.

Denton, J.D. (1993). Loss Mechanisms in Turbomachines.
ASME J. Turbomach., 115, pp.621-656.

Eulitz. F., Engel, K. and Gebing, H., (1996). *Numerical Iinvestigation of the Clocking Effects in a Multistage Turbine*, Proc. Int. Gas Turbine Aeroengine Congr. Exhib., Vol. 96-GT-26, 1996.

Evans, K.R. and Longley., J.P., (2016a). *Accounting for Uncontrolled Variations in Low-Speed Turbine Experiments*. paper GT2016-56667, Proceedings of ASME Turbo Expo 2016, June 13 – 17, 2016, Seoul, South Korea

Evans, K.R. and Longley., J.P., (2016b). *Clocking in Low Pressure Turbines*. paper GT2016-56668, Proceedings of ASME Turbo Expo 2016, June 13 – 17, 2016, Seoul, South Korea

Fischer, S. (2011). *Untersuchung ebener Verdichtergitter mit aktiver Zirkulationskontrolle an der Hinterkante*. PhD Thesis, Technische Universität Braunschweig.

Göttlich, E. (2011)*, Research on the Aerodynamics of Intermediate Turbine Diffusers.* Progress in Aerospace Sciences, doi:10.1016/j.paerosci.2011.01.002.

Goldstein, S. (1938). Modern developments in fluid dynamics.
Proc. R. Soc. Lond. 155, 570–575.

Khalid, S.A; , Khalsa, A.S., Waitz, I.A., Choon, S.T., Greitzer, E.M., Cumpsty, N., Adamczyk, J.J.., Marble, F.E., (1998). *Endwall Blockage in Axial Compressors*, ASME-Paper 98-GT-188.

Koch, H., Kozulovic, D., Hoeger, M. (2012). *Outlet Guide Vane Airfoil for Low Pressure Turbine Configurations*. 42nd AIAA Fluid Dynamics Conference, June 2012, New Orleans, Louisiana, USA

Kozulovic, D., (2007). Modellierung des Grenzschichtumschlags bei Turbomaschinen-strömungen unter Berücksichtigung mehrerer Umschlagsarten. PhD thesis,
Ruhr-Universit¨at Bochum and DLR Forschungsbericht 2007-20.

Kurz, J., Hoeger, M., Niehuis, R. (2017). Active Boundary Layer Control on a highly loaded Turbine Exit Case profile. paper ETC2017- 191, to be presented on 12th European Turbomachinery Conference, 3.-7. April 2017 Stockholm, Sweden.

Marn, A., Göttlich, E., Cadrecha, D., Pirker, H.-P. (2009). *Shorten the Intermediate Turbine Duct Length by Applying an Integrated Concept.* ASME Journal of Turbomachinery, 131, 041014.

Marn, A., Broszat, D., Selic, T., Schönleitner, F., Heitmeir, F. (2015). *Comparison of the Aerodynamics of Acoustically Designed EGVs and a State-of-the-Art EGV*. ASME Journal of Turbomachinery, 137, 041002.

Michelassi,V,, Chen, L., Pichler, R., Sandberg, R., Bhaskaran, R. (2015). *High-Fidelity Simulations of Low-Pressure Turbines: Effect of Flow Coefficient and Reduced Frequency on Losses*. ASME paper GT2015-43429. Proceedings of ASME Turbo Expo, June 15-19, 2015, Montreal, Canada.

Moser, M., Kahl, G., Kulhanek, G. and Heitmeir, F. (2007). Construction of a Subsonic Test Turbine Facility for Experimental Investigations of Sound Generation and Propagation for Low Pressure Turbines. Beijing, China, ISABE-2007-1366.

Nerger, D. (2009). *Aktive Strömungsbeeinflussung in ebenen Statorgittern hoher aerodynamischer Belastung durch Ausblasen*. PhD Thesis, Technische Universität Braunschweig.

Santner, C., Paradiso B., Malzacher F., Hoeger M., Hubinka J., Göttlich E. (2011). Evolution of the Flow Through a Turning Mid Turbine Frame Applied Between a Transonic HP-Turbine Stage and a Counter-Rotating LP-Turbine. 9th European Turbomachinery Conference, 21-25. March, 2011, Istanbul, Turkey.

Schönleitner, F., Koch, H., Selic, T., Hoeger, M., Marn,A. (2014). *Comparison of the Experimental Results Between a 2D EGV Cascade Test and a Rig Test Under Engine Representative Conditions*. ASME Paper GT2014-26915, Proc. of the ASME Turbo Expo, Düsseldorf, Germany.

Stieger, R.D., Hodson, H.P., (2004). *The Unsteady Development of a Turbulent Wake Through a Downstream Low-Pressure Turbine Blade Passage.* ASME-paper GT2004-53061, Proceedings of ASME Turbo Expo, 2004, June 14-17, 2004, Vienna, Austria.

Sturm, W. and Fottner, L. (1985) The High-Speed Cascade Wind-Tunnel of the German Armed Forces Munich. In 8th Symposium on Measuring Techniques for Transonic and Supersonic Flows in Cascades and Turbomachines. Genova, Italy

APPENDIX 1: TURBULENCE AND PROBE READING

Little is published on the impact of unsteady flow conditions on probe reading. As given in an early work of Goldstein (1938), a Pitot probe senses not vector components but the total pressure scalar $Pt = p + \rho/2\ (U_o^2+u'^2+v'^2+w'^2)$ with U_o in main flow direction and fluctuation u'. Using only the components v' and w' at constant static pressure, we get for the increase in Pitot reading from turbulence with dynamic head $q=\rho/2U_o^2$:

$$\Delta Pt/q = 2\ Tu^2. \qquad \text{eq. (A1)}$$

Results from equation (A1) are given in Fig. A1. Using measured TEC inlet stochastic data with Tu_1 = 5 to 6 % a total pressure increase of 0.6 % q is felt by the probe from turbulence.

Similar to turbulence, probe oscillations may impact the probe reading. However it is pointed out in Bailey et al. (2013) that Goldsteins's formula is not an accepted universal relation. To exclude any probe specific deviations, a miniature Pitot probe was manufactured by University of Technology Graz for the present investigations. Furthermore in Bauinger et al. (2017) 5-hole probe and unsteady FRAP-probe data are demonstrated to fit even at high frequencies and high Tu_1 beyond 5%.

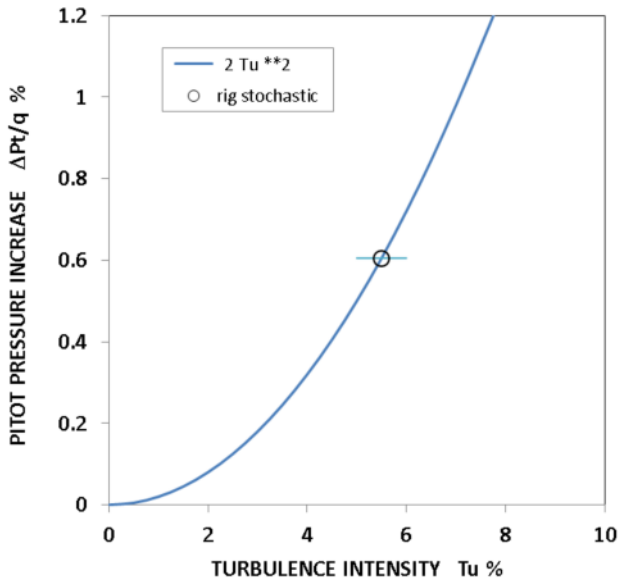

Figure A1: Increase in Pitot total pressure with turbulence intensity at TEC inlet